

# Class A small area solar simulator for dye-sensitized solar cell testing

A. GEORGESCU, G. DAMACHE, M. A. GÎRȚU\*

*Department of Physics, Ovidius University of Constanța, Constanța 900527, Romania*

The need for high quality solar simulators for photovoltaic device testing is an increasing demand, given the more severe requirements for accuracy and reproducibility of cell efficiency measurements. This paper describes a homemade small area solar simulator using both a xenon lamp and a halogen lamp and the appropriate set of filters to correctly replicate the solar spectrum. We show that all three characteristics required by the ASTM Standard E927-05 for a class AAA solar simulator, namely spectral match, spatial non-uniformity and temporal instability, are met. We demonstrate the possibility to measure the current-voltage curve under  $100 \text{ mWcm}^{-2}$  standard AM 1.5 G spectrum (International Electrotechnical Commission 60904-1) as well as at various levels of irradiation up to 1.2 suns and in a temperature range from 5 - 55°C, using a dye-sensitized solar cell with nanocrystalline  $\text{TiO}_2$  and a ruthenium-based dye.

(Received September 1, 2008; accepted October 30, 2008)

**Keywords:** Solar simulation, Solar cell, Dye-sensitized cell,  $\text{TiO}_2$ , Ruthenium-based dye

## 1. Introduction

Solar simulators can have wide applications, from testing products such as sunscreen and studying UV degradation in plastics, but their most important application is in the characterization and certification of photovoltaic (PV) cells. The recent increase in the photovoltaic market [1] has triggered a high growth rate of the number of publications on organic solar cells (OSC) and hybrid organic-inorganic solar cells (HOISC). In a position paper Dennler and co-signatories [2] note the significant number of articles claiming unrealistic and scientifically questionable OSC properties and performances and recommend that the process of measuring the OSC efficiency follows the specific protocol [3,4].

Regardless of design and active material, PV cells are all subject to the same standard test conditions. The cells are typically insolated at a constant density of roughly  $1000 \text{ W/m}^2$ , which is defined as the standard “1 Sun” value, with spectrum consistent to an air-mass (AM) global value of 1.5 (AM 1.5G), at an ambient temperature of 25°C. In addition to these standard test conditions, international standards such as IEC 904-9, JIS C 8912-1989, and ASTM E927-05 define three classes of solar simulation performance-classes A, B, and C. The highest certification level is Class A, whose requirements do not vary significantly among the three international standards. By ensuring measurement uniformity that allows results comparability and traceability, Class A systems reduce the process variability of photovoltaic cell testing as compared to lower class sources.

The classification of a solar simulator depends on the size of the test plane. If the test plane is smaller or equal to  $30 \times 30 \text{ cm}$ , that is a small area simulator and the constraints imposed to such systems are stronger than for large area simulators (see Table 1) [5]. The main requirements for

solar simulators regard the spectral match, spatial non-uniformity, and temporal instability [5]. Therefore a complete classification of a solar simulator must contain all three criteria. Many times, however, class A simulator is a shorter description meaning that the simulator is rated A in all three classes.

*Table 1. Specifications for solar simulators according to the ASTM E927-05 standard [5].*

Area	Classification	Characteristics		
		Spectral match	Spatial non-uniformity	Temporal instability
Small Area	Class A	0.75 to 1.25	2 %	2 %
	Class B	0.6 to 1.4	5 %	5 %
	Class C	0.4 to 2.0	10 %	10 %
Large Area	Class A	0.75 to 1.25	3 %	2 %
	Class B	0.6 to 1.4	5 %	5 %
	Class C	0.4 to 2.0	10 %	10 %

The spectral match is important because it ensures that test conditions match real-world conditions and eliminate variability from batch-to-batch testing. Spatial uniformity – probably the most difficult specification to achieve, especially for large area simulators - minimizes “hot spots” that can distort cell performance testing and repeatability. Temporal stability dictates that lamp fluctuations do not distort measurement of solar-cell efficiency.

Solar simulator design has evolved greatly in recent years. Manufacturers have been searching for better light sources and improved filters as well as new designs to better match the reference spectrum [6]. If traditional light sources were tungsten halogen lamps, more recently xenon lamps have been extensively used due to their higher output, lower consumption and stronger emission in the low wavelength part of the spectrum. It was pointed out, however, that the efficiency with respect to standard reporting conditions cannot be determined with a single light source [3,7]. Multiple source solar simulators have been built to improve the spectral match [8,9], one of the key challenges being the appropriate filtering of the light sources [10].

We report here on a homemade solar simulator using two lamps, one with xenon and the other with halogen, and the appropriate set of filters to correctly replicate the solar spectrum. We show that all three characteristics required by the ADTM Standard E927-05 for a class AAA solar simulator, spectral match, spatial non-uniformity and temporal instability are met for a circular slit with a diameter of 10 mm, used for testing dye sensitized solar cells. We demonstrate the possibility to measure the current-voltage curve under 100  $\text{mWcm}^{-2}$  standard AM 1.5 G (AM: air mass) spectrum (International Electrotechnical Commission 69094-1) as well as at various levels of irradiation up to 1.2 suns and in a temperature range from 5 - 55°C, using a dye-sensitized solar cell (DSSC) with nanocrystalline  $\text{TiO}_2$  and a ruthenium-based dye.

## 2. Experimental

The solution chosen for our solar simulator is based on a combination of two light beams from two independent sources, each with its one voltage supply and appropriate optical filters. The advantage of this solution is that it allows a good spectral match to the solar reference by mixing the strong low wavelength beam of a xenon discharge lamp with the high IR contribution of a tungsten halogen lamp.

The schematic layout of the experimental setup is displayed in Fig. 1. The optical system is based on two discontinued photographic slide projectors, originally equipped with a fan-cooled incandescent light bulb, a reflector and a condenser to direct the light to the slide, a holder for the slide and a focusing lens. The mirrors were removed to improve spatial uniformity of the beams. Particularly useful was the heat absorbing glass placed in the light path between the condensing lens and the photographic slide to protect the latter. The glass transmits visible wavelengths but absorbs infrared eliminating the need of additional filters.

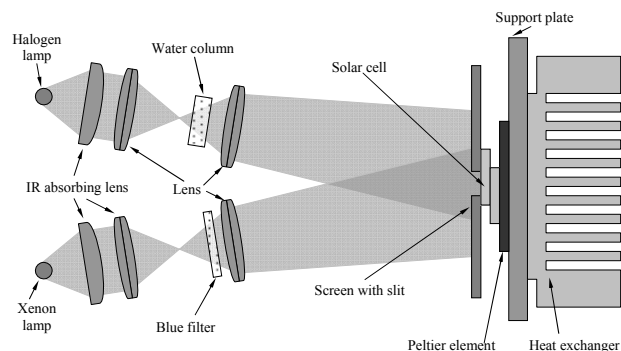


*Fig. 1. Optical layout of the solar simulator. The beams from two independent lamps, each mounted in a photographic slide projector, pass through condenser lenses, filters and magnifying lenses to overlap on a screen. Behind the screen, the PV device is in thermal contact with a Peltier element connected to a temperature regulator.*

The area where the two beams overlap is about  $4 \times 3 \text{ cm}^2$ . The PV devices are mounted on a sample holder with a Peltier element allowing measurements at controlled temperatures. The model used can provide a temperature separation between the two sides of 75°C at a maximum dissipated power of 57 W, maximum current of 6.4 A for and voltage of 16.4 V. The temperature is stabilized using a temperature regulator, not shown.

The halogen lamp used is a regular 55 W – 12 V headlight tungsten halogen lamp, which is an incandescent lamp with a tungsten filament sealed into a compact transparent envelope filled with an inert gas and a small amount of halogen such as iodine or bromine. Fig. 2 displays a comparison between the solar spectrum and the spectra taken for the lamp without as well as with the IR absorbing lens, all measured with an Ocean Optics HR4000CG-UV-NIR spectrometer, calibrated with an optical fiber and an integrating sphere, in the Absolute Irradiance mode. It can be seen that the filtering effect of the IR absorbing lens is very effective in bringing the spectrum of the lamp closer to the solar one. One can note that a large difference between the solar and the halogen lamp spectrum occurs approximately near 930 and 970 nm, likely caused by the absorption of light in the water vapors in the atmosphere [11]. To better describe this part of the spectrum we inserted a water column placed in spectroscopic glass into the path of the halogen lamp light beam. As it can be seen from Fig. 2, the spectral match was considerably improved in the region around 970 nm.

The xenon lamp used is a 35 W – 35 kV (with a 12 V power supply) Kaixen high intensity discharge lamp with a color temperature of 6000 K. Figure 3 displays the solar spectrum and the spectra of the lamp beam with the IR absorbing lens and with both the IR filtering lens and the blue plastic filter. The measurements were taken using the smoothing option of the spectrometer (the value of each point is an average that also takes into account next 10 points on each side). It can be seen that most of the light emitted by the xenon lamp is in the 350-600 nm region of

the spectrum. The IR absorbing lens is useful in this case too, cutting some of the sharp peaks of the xenon lamp around 671, 821, 882, 9005 and 917 nm.

The removal of the IR part of the spectrum of the xenon lamp is compensated by the good spectral match in that region of the halogen lamp.

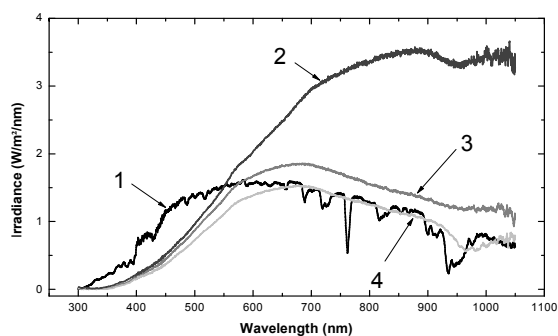


Fig. 2. Solar spectrum (1), together with the spectra of the halogen lamp without (2) and with (3) the IR absorbing lens, and with both the IR-cutting lens and the water column (4).

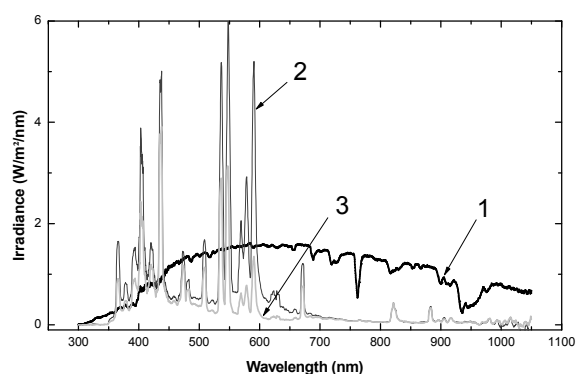


Fig. 3. Solar spectrum (1), xenon lamp with infrared-cutting lens (2) and xenon lamp with infrared-cutting lens and blue filter (3).

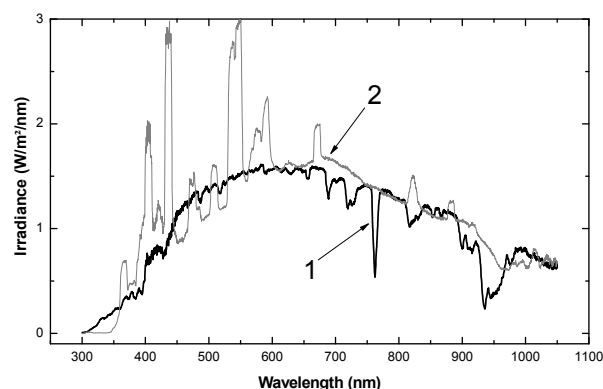


Fig. 4. Complete simulator spectrum (2), compared with the solar spectrum (1)

### 3. Calibration

#### 3.1 Spectral match

The IEC 904-9, JIS C 8912-1989, and ASTM E927-05 standards define the spectral match of a solar simulator as a percentage of the integrated intensity over 6 spectral ranges. Any deviation from the specified percentages must then lie within a range that determines the class of the simulator. The total irradiance measured with both beams is displayed together with the solar spectrum in Fig. 4. The exact errors of this spectrum are analyzed in the next section.

Spectral distribution of irradiance performance requirements for class A as defined in ASTM E927-05, together with the measurements of our solar simulator are shown in table 2. All the spectral ranges of our simulator are within the accepted limits for class A simulators. Figure 5 shows the variation of the irradiance percentage of our simulator, compared with the upper and lower limit for class A devices.

Table 2 Requirements for the distribution of irradiance for class A solar simulators, as defined in ASTM E927-05 and the results for our simulator.

Range (nm)	400/500	500/600	600/700	700/800	800/900	900/1100
Simulator:						
Measured %	14.08	19.86	18.21	16.34	14.08	14.59
Class A (allows tolerances of $\pm 25\%$ of ideal)						
Min %	13.8	14.9	13.8	11.2	9.3	11.9
Ideal %	18.4	19.9	18.4	14.9	12.5	15.9
Max %	23	24.8	23	18.6	15.6	19.9

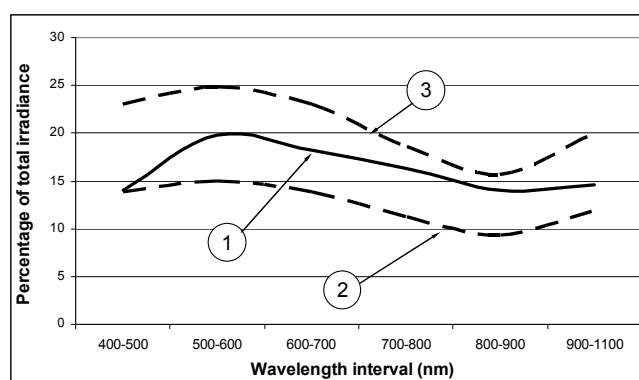


Fig. 5. Percentages of: simulator (1), class A lower limit (2) and class A upper limit (3).

#### 3.2 Spatial non-uniformity

Spatial non-uniformity on the test plane can be calculated with the following formula:

$$S_{NE} = 100\% \times \frac{E_{\max} - E_{\min}}{E_{\max} + E_{\min}},$$

where  $E_{\max}$  and  $E_{\min}$  are measured with the detector over the test plane area.

The total non-uniformity that we calculated from our measurements over the small test area is less than 0.5%, while the one accepted for a class A simulator is 2%. A schematic with the percentages of the measured values related to the value in the center of the slit is shown in Figure 6.

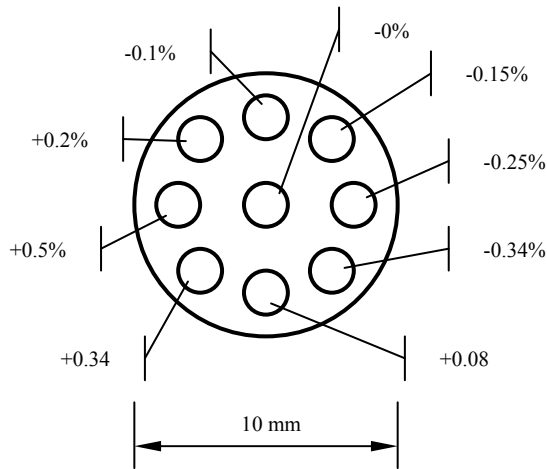


Fig. 6. Percentages of the values measured within the 10 mm diameter slit, with respect to the value in the center.

### 3.3 Temporal non-uniformity

Temporal instability can be calculated with the following formula:

$$T_{IE} = 100\% \times \frac{E_{\max} - E_{\min}}{E_{\max} + E_{\min}},$$

where  $E_{\max}$  and  $E_{\min}$  are measured with the detector at any point on the test plane during the time of data acquisition. The temporal instability calculated for an interval of one hour was 1,17%, whereas the accepted value is 2%.

## 4. Testing

After calibration, the solar simulator was used as a reference light source for testing dye-sensitized solar cells [12-15]. The solar cells were firstly prepared using the method described in the next lines.

For preparation of nanocrystalline  $\text{TiO}_2$  photoelectrode, a small amount of  $\text{TiO}_2$  suspension (Ti nanoxide-T: colloidal anatase, particle size of ~13 nm,

Solaronix, Switzerland) was applied onto a conductive glass by doctor blading using adhesive tape (thickness ~50  $\mu\text{m}$ ) as a frame and spacer. The conductive glass substrate (Solaronix) consisted of a soda lime glass sheet of 2.2 mm thickness, with a conductive layer of F-doped  $\text{SnO}_2$  (sheet resistance: 15  $\Omega/\text{square}$ ). Optical transmission is greater than or equal to 80% in the 400-700 nm region. After evaporation of solvent from the deposited suspension, the substrate with the obtained film was sintered for 30 minutes at 450°C in the oven. The resulting plate was then immersed into the dye solution and then washed to remove any dye that hasn't been absorbed by the  $\text{TiO}_2$  layer. The counter electrode consisted of a thermally platinized conductive glass, 5 mM  $\text{H}_2\text{PtCl}_6$  (Solaronix) in dry isopropanol, heated at 380°C on the same type of conductive glass substrate for 10 minutes. The two described above electrodes were clipped together to make a sandwich type cell. The electrolyte was injected into the space between the electrodes and filled the nanocrystalline  $\text{TiO}_2$  layer through a capillary action. The electrolyte solution was an iodide based high boiling point electrolyte with 50 mM of tri-iodide in Tetraglyme (TG-50, Solaronix). The cell measurements were performed using a precision decadic resistance box and two digital bench multimeters, model Mastech MS8050.

The temperature dependence of the current-voltage curve at various temperatures for the DSSC studied is shown in Fig. 7. We note that on increasing the temperature from 5°C to 55°C the open-circuit voltage increases whereas the short-circuit current density decreases. Of all the curves taken under standard AM 1.5G solar irradiation conditions, only the curve at 25°C can provide a reliable value for the fill factor and the overall device efficiency.

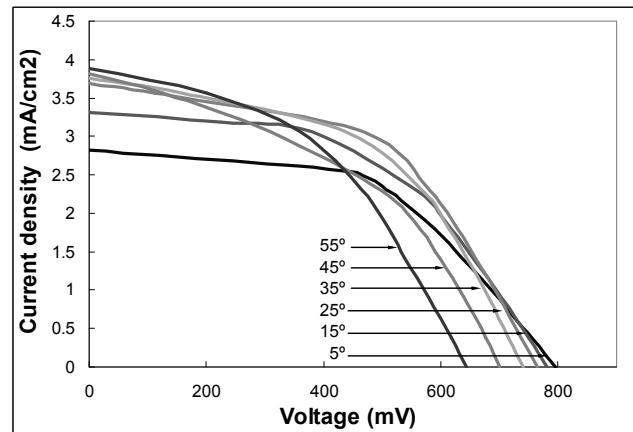


Fig. 7. I-V curves at temperatures between 5 and 55°C under standard AM 1.5G illumination conditions for a DSSC based on nanocrystalline  $\text{TiO}_2$  sensitized with a ruthenium dye

Fig. 8 shows the current-voltage curves of the DSSC under different illumination intensities, at a temperature of 25°C. As expected, a higher irradiance leads to a larger short-circuit current density. It can be seen that the short-circuit current density varies almost linearly with the

illumination, roughly, to a 12 times increase in irradiance corresponding about a 12 times increase in current density.

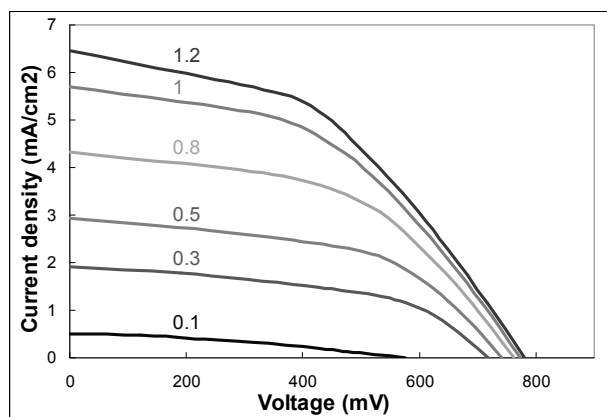


Fig. 8. Current density-voltage curves of a DSSC based on nanocrystalline  $\text{TiO}_2$  sensitized with a ruthenium dye at irradiance values varying from 0.1 to 1.2 sun, at  $25^\circ\text{C}$ .

## 5. Conclusions

We reported the design and implementation of a homemade solar simulator using two light sources, a xenon discharge lamp and a halogen lamp and the appropriate set of filters to correctly replicate the solar spectrum. We showed that the three characteristics required by the ASTM Standard E927-05 for a class AAA solar simulator, namely the spectral match, the spatial uniformity and the temporal stability are all met. We demonstrated that the possibility to control the device temperature over the range  $5\text{--}55^\circ\text{C}$  as well as the irradiance between 0.1 and 1.2 suns opens a wide range of measurements to be performed on dye-sensitized solar cells, as well as other photovoltaic devices.

## Acknowledgments

We gratefully acknowledge the financial support from the Romanian Ministry of Education and Research through the CNCSIS grant A678/2006 and the ANCS grant CEEX-M3-C3-12350/2006. The authors are thankful to dr. Amir Baranzahi, from Linköping University for useful discussions.

## References

- [1] A. Jäger-Waldau, PV Status report 2006, Office for Official Publications of the European Communities Luxembourg, 2006.
- [2] G. Dennler, *Materials Today* **10**, 56 (2007).
- [3] K. Emery, C. Osterwald, in *Current Topics in Photovoltaics*, vol. 3, chapt. 4, Academic Press, London, UK, 1988.
- [4] V. Shrotriya et al., *Adv. Funct. Mater.* **16**, 2016 (2006).
- [5] ASTM Standard E927-05, Standard Specification for Solar Simulation for Photovoltaic Testing, ASTM International, West Conshohocken, PA, USA, [www.astm.org](http://www.astm.org).
- [6] ASTM Standard G173-03e1 - Standard Tables for Reference Solar Spectral Irradiances: Direct Normal and Hemispherical on  $37^\circ$ , ASTM International, West Conshohocken, PA, USA, [www.astm.org](http://www.astm.org).
- [7] K. Emery, C.R. Osterwald, T. Glatfelter, J. Burdick G. Virshup, *Solar Cells* **24**, 371 (1988).
- [8] F. Nagamine, R. Shimokawa, M. Suzuki, T. Abe, *Conf. Rec. IEEE Photovoltaic Spec. Conf.* **23**, 686 (1993).
- [9] V. A. Wilkinson, C. Goodbody, *Conf. Rec. IEEE Photovoltaic Spec. Conf.* **26**, 947 (1997).
- [10] K. Emery, D. Myers, S. Rummel, *Conf. Rec. IEEE Photovoltaic Spec. Conf.* **20**, 1087 (1988).
- [11] P. F. Bernath, *Phys. Chem. Chem. Phys.* **4**, 1501 (2002).
- [12] B.O'Regan and M. Gratzel, *Nature* **335**, 737 (1991).
- [13] M. Gratzel, *J. Photochem. Photobiology A: Chem.* **164**, 3 (2004); M. Grätzel, *Inorg. Chem.* **44**, 6841 (2005).
- [14] A. Kanciurzevska, E. Dobruchowska, A. Baranzahi, E. Carlegrim, M. Fahlman, and M.A. Gîrțu, *J. Optoelectron. Adv. Mater.* **9**, 1052 (2007).
- [15] A. Dumbravă, A. Georgescu, G. Damache, C. Badea, I. Enache, C. Oprea and M.A. Gîrțu, *J. Optoelectron. Adv. Mater.*, **10**(11), 2996 (2008).

\*Corresponding author: [girtu@univ-ovidius.ro](mailto:girtu@univ-ovidius.ro)